Available online at www.sciencedirect.com
ScienceDirect
Journal of Solid State Chemistry 180 (2007) 1799–1808
JOURNAL OF SOLID STATE CHEMISTRY
www.elsevier.com/locate/jssc

Four new hydroxymonophosphates with closely related intersecting tunnels structures: The series $AM^{III}(PO_3(OH))_2$ with $A = Rb, Cs$; $M = Fe, Al, Ga, In$

J. Lesage, L. Adam, A. Guesdon*, B. Raveau

Laboratoire CRISMAT, UMR 6508 CNRS ENSICAEN, 6 bd Maréchal Juin, 14050 CAEN Cedex, France

Received 12 February 2007; received in revised form 4 April 2007; accepted 6 April 2007
Available online 14 April 2007

Abstract

The family of hydroxymonophosphates of generic formula $AM^{III}(PO_3(OH))_2$ has been revisited using hydrothermal techniques. Four new phases have been synthesized: $CsIn(PO_3(OH))_2$, $RbFe(PO_3(OH))_2$, $RbGa(PO_3(OH))_2$ and $RbAl(PO_3(OH))_2$. Single crystal diffraction studies show that they exhibit two different structural types from previously observed other phases with $A = H_3O$, NH_4, Rb and $M =$ Al, V, Fe. The "Cs–In" and "Rb–Fe" phosphates crystallize in the triclinic space group $P\bar{1}$, with the cell parameters $a = 7.4146(3)$ Å, $b = 9.0915(3)$ Å, $c = 9.7849(3)$ Å, $\alpha = 65.525(3)^\circ$, $\beta = 70.201(3)^\circ$, $\gamma = 69.556(3)^\circ$ and $V = 547.77(4)$ Å^3 ($Z = 3$) for $CsIn(PO_3(OH))_2$ and $a = 7.2025(4)$ Å, $b = 8.8329(8)$ Å, $c = 9.4540(8)$ Å, $\alpha = 65.149(8)^\circ$, $\beta = 70.045(6)^\circ$, $\gamma = 69.591(6)^\circ$ and $V = 497.44(8)$ Å^3 ($Z = 3$) for α-$RbFe(PO_3(OH))_2$. The "Rb–Al" and "Rb–Ga" phosphates crystallize in the $R\bar{3}c$ space group, with $a = 8.0581(18)$ Å and $c = 51.081(12)$ Å ($V = 2872.5(11)$ Å^3 and $Z = 18$) for $RbAl(PO_3(OH))_2$ and $a = 8.1188(15)$ Å and $c = 51.943(4)$ Å ($V = 2965(8)$ Å and $Z = 18$) for $RbGa(PO_3(OH))_2$. These two structural types are closely related. Both are built up from $M^{III}O6$ octahedra sharing their apices with $PO_3(OH)$ tetrahedra to form $[M_3(PO_3OH)_6]$ units, but the latter exhibits a different configuration of their tetrahedra. The three-dimensional host-lattices result from the connection of the $[M_3(PO_3OH)_6]$ units and they present numerous intersecting tunnels containing the monovalent cations.

Keywords: Hydroxymonophosphates; Hydrothermal synthesis; Single crystal X-ray diffraction; Structure determination; Intersecting tunnel structure; Mixed framework

1. Introduction

The remarkable ability of the phosphate frameworks to accommodate various structural units, and especially octahedral ones, makes that a tremendous number of phosphate derivatives can be generated. The research of the latter is of great interest since, depending on the nature of the polyhedra associated to the phosphate groups, a large variety of properties and applications can be designed, such as ionic conductivity [1–4] and molecular sieves [5,6] in open frameworks materials, or redox catalytic properties in phosphates of mixed valent transition elements [7,8], or even trapping of radioactive cations for the storage of nuclear wastes [9–11]. In this respect, the family of indium phosphates still offers a wide field for exploration, since less than about fifty indium phosphates or hydroxyphosphates containing besides indium a second element are actually known. We have revisited the Cs–P–In–O system for which three phases only are known to date, the phosphates $CsInP_2O_7$ [12] and $Cs_3In_3P_{12}O_{36}$ [13] and the hydroxyphosphate $CsIn_2(PO_4)(HPO_4)_2(H_2O)_2$ [14]. We have thus synthesized for the first time a cesium indium hydroxyphosphate, $CsIn(PO_3(OH))_2$, which presents a triclinic structure isotypic with that of α-$RbV(PO_3(OH))_2$ [15], $NH_4V(PO_3(OH))_2$ [16], $NH_4(Al_{0.64}Ga_{0.36})(PO_3(OH))_2$ [17], $H_3OAl(PO_3(OH))_2$ [18] and $NH_4Fe(HPO_4)_2$ [19]. Attempts to obtain this structural type for other monovalent and trivalent cations allowed three other compounds to be synthesized: α-$RbFe(PO_3(OH))_2$, which crystallizes

*Corresponding author. Fax: +33 2 31 95 16 00.
E-mail address: anne.guesdon@ensicaen.fr (A. Guesdon).

0022-4596/$ - see front matter © 2007 Elsevier Inc. All rights reserved.
doi:10.1016/j.jssc.2007.04.005

with the same triclinic structure type, and $RbGa(PO_3(OH))_2$ and $RbAl(PO_3(OH))_2$ which both adopt a structure with a trigonal symmetry, isotypic with that of $RbFe(PO_3(OH))_2$ [20].

We report thus herein on the hydrothermal syntheses and the crystal structures of these four new hydroxyphosphates. Both studied frameworks exhibit large intersecting tunnels and they exhibit close structural relationships since they are built from similar $M_3O_6[PO_3(OH)]_6$ (M = In, Fe, Ga or Al) basic units. From the positions of the hydrogen atoms, we observe the existence of strong hydrogen bonds which reinforce the stability of the structure.

2. Synthesis and crystal growth

The single crystals used for the structure determinations of the four studied compounds ($CsIn(PO_3(OH))_2$ (**1**), α-$RbFe(PO_3(OH))_2$ (**2**), $RbGa(PO_3(OH))_2$ (**3**) and $RbAl(PO_3(OH))_2$ (**4**)) were extracted from four different batches. They were prepared by hydrothermal synthesis performed in 21 ml Teflon-lined stainless steel Parr autoclaves in the following way.

An aqueous solution of AOH (50% diluted solutions, Alfa Aesar, 99% for A = Cs and 99.6% for A = Rb) was first mixed with H_3PO_4 (85%, Prolabo Rectapur) and deionized water (2 ml for **1**, **2** and **3** and 0.5 ml for **4**). The $M_2^{III}O_3$ oxide (Chempur 99.99% for M = In, Carlo Erba 99% for M = Al, Alfa Aesar 99.99% for M = Ga and Merck 99% for M = Fe) was then added to the acidic solution. For the iron-containing synthesis, $FeCl_2$ (Alfa Aesar 99.5%) was also added. The cationic A:M:P proportions in the so prepared mixtures were 1:2:2 for M = In and M = Fe (with 1:2 molar proportion for Fe_2O_3:$FeCl_2$), 5:6:9 for M = Ga, and 1:1:2 for M = Al. The total mass of precursors (without taking water into account) was of ca. 0.8 g for **1**, **3** and **4** and of ca. 1.1 g for **2**. The iron-containing preparation (pH ≈ 2) was heated at 220 °C for 25 h, then cooled down to room temperature for 17 h. The three other preparations (pH ≈ 2) were heated at 200 °C for 24 h, then cooled down to room temperature for 18 h. Each product was filtered off and washed with water, leading for the indium-containing preparation to a yellow powder, for the aluminium and gallium ones to white powders and for the iron one to a green powder. The careful examinations of these preparations revealed for all of them the presence of small colourless crystals which could be identified as the four title compounds after the studies described in the following sections.

Attempts were performed in order to obtain monophasic samples for each of the four studied compounds. Although the use of different syntheses conditions (i.e. different precursors, temperatures, heating cycles, or concentrations), the examination of the XRD patterns of the obtained polycrystalline powders systematically revealed the presence of a small amount of at least one secondary phase in the batch. (Fe_2O_3 for the α-$RbFe(PO_3(OH))_2$ syntheses, performed without using $FeCl_2$, In_2O_3 for $CsIn(PO_3(OH))_2$, and leucophosphite-type phases for $RbGa(PO_3(OH))_2$ and $RbAl(PO_3(OH))_2$). Note that the triclinic polymorphs could be synthesized without the trigonal one for α-$RbFe(PO_3(OH))_2$ and $CsIn(PO_3(OH))_2$ and that, similarly, no triclinic polymorph was observed in the $RbGa(PO_3(OH))_2$ and $RbAl(PO_3(OH))_2$ syntheses batches.

3. Crystal studies: EDX analysis and X-ray diffraction

The semi-quantitative analyses of the crystals extracted from the preparations were performed with an OXFORD 6650 microprobe mounted on a PHILIPS XL30 FEG scanning electron microscope. The obtained cationic compositions were in agreement with the expected theoretical values of "25:25:50", respectively for the A, M and P elements (experimental values : "23:24:53" for Cs:In:P (**1**), "21:21:58" for Rb:Fe:P (**2**), "25:21:54" for Rb:Ga:P (**3**) and "22:22:56" for Rb:Al:P (**4**).

A colorless crystal was chosen in each of the four preparations for the single crystal X-ray diffraction studies, which were performed at 293 K with a Bruker-Nonius Kappa CCD four-circle diffractometer equipped with a two-dimensional CCD detector and using the Mo$K\alpha$ radiation. Data were collected with the data collection parameters reported in Table 1. They were reduced and corrected for Lorentz and polarization effects with the Eval CCD package [21]. The cell parameters indicated in Table 1 were accurately refined from the whole registered frames. Absorption correction, structure determination, refinement and secondary extinction correction were performed for the four studied crystals, with the JANA 2000 program [22].

The structure of $CsIn(PO_3(OH))_2$ **(1)** was solved in the centrosymmetric $P\bar{1}$ space group, using the heavy atom method and successive difference Fourier syntheses and Fourier syntheses. In a first time, Cs, In, P and O atoms were localized. The refinement of their atomic coordinates and anisotropic thermal parameters led to the reliability factors $R = 0.0313$ and $Rw = 0.0348$. The maximum of residual electronic densities was $0.94\,e^-.Å^{-3}$. The chemical formula for the cell content deduced from this refinement, "$Cs_3In_3(PO_4)_6$", suggested that six positive charges per cell unit were missing to ensure the charge balance. Bond valence sum (BVS) calculations [23] were thus performed at this stage of the refinement. The calculated values for cesium, indium, phosphorus cations and O(1) to O(9) oxygen anions were close to the theoretical values of 1, 3, 5 and 2, respectively whereas O(10), O(11) and O(12) had respective BVS values of 1.23, 1.27 and 1.28 (Table 2). These calculations thus indicate the presence of three hydroxyl groups, leading for compound **1** to the chemical formula $CsIn(PO_3(OH))_2$ ($Z = 3$) for which charge balance is respected. In order to localize the corresponding hydrogen atoms, difference Fourier maps were calculated with reflections of low θ diffraction angles (from 5° to about 20°). From their examination, three hydrogen atoms could be localized at about 0.80 Å from O(10), O(11) and

Table 1
Summary of single crystals data, intensity measurements and structure refinement parameters

	$CsIn(PO_3(OH))_2$ **(1)**	α-$RbFe(PO_3(OH))_2$ **(2)**	$RbGa(PO_3(OH))_2$ **(3)**	$RbAl(PO_3(OH))_2$ **(4)**
1. *Crystal data*				
Crystal dimensions:	$0.059 \times 0.033 \times 0.015\,mm^3$	$0.103 \times 0.026 \times 0.013$	$0.097 \times 0.087 \times 0.071\,mm^3$	$0.101 \times 0.084 \times 0.044\,mm^3$
Space group	P–1	P–1	R–3 c	R–3 c
Cell dimensions	$a = 7.4146(3)$ Å	$a = 7.2025(4)$ Å	$a = 8.1188(15)$ Å	$a = 8.0581(18)$ Å
	$b = 9.0915(3)$ Å	$b = 8.8329(8)$ Å		
	$c = 9.7849(3)$ Å	$c = 9.4540(8)$ Å	$c = 51.943(4)$ Å	$c = 51.081(12)$ Å
	$\alpha = 65.525(3)^\circ$	$\alpha = 65.149(8)^\circ$		
	$\beta = 70.201(3)^\circ$	$\beta = 70.045(6)^\circ$		
	$\gamma = 69.556(3)^\circ$	$\gamma = 69.591(6)^\circ$		
Volume	$547.77(4)\,Å^3$	$497.44(8)\,Å^3$	$2965.1(8)\,Å^3$	$2872.5(11)\,Å^3$
z	3	3	18	18
Formula weight	$439.7\,g\,mol^{-1}$	$333.3\,g\,mol^{-1}$	$347.1\,g\,mol^{-1}$	$304.4\,g\,mol^{-1}$
ρ calc	$3.9973(3)\,g\,cm^{-3}$	$3.3365\,g\,cm^{-3}$	$3.4983\,g\,cm^{-3}$	3.1655 g cm−3
2. *Intensity measurements*				
λ(Mo*K*α)	0.71069 Å	0.71069 Å	0.71069 Å	0.71069 Å
Scan strategies				
	φ and ω scans	φ and ω scans	φ and ω scans	φ and ω scans
	0.5°/frame	0.8°/frame	0.5°/frame	0.5°/frame
	60 s/°	120 s/°	240 s/°	180 s/°
	2 iterations	2 iterations	2 iterations	2 iterations
	Dx = 34 mm	Dx = 38 mm	Dx = 34 mm	Dx = 34 mm
θ range for data collection and limiting indices	$5.94^\circ \leqslant \theta \leqslant 39.99^\circ$	$5.82^\circ \leqslant \theta \leqslant 38.99^\circ$	$5.85^\circ \leqslant \theta \leqslant 39.99^\circ$	$5.90^\circ \leqslant \theta \leqslant 39.99^\circ$
	-13	$-12 \leqslant h \leqslant 12$	$-14 \leqslant h \leqslant 9$	$-14 \leqslant h \leqslant 11$
	$-16 \leqslant k \leqslant 16$	$-15 \leqslant k \leqslant 15$	$-9 \leqslant k \leqslant 14$	$-8 \leqslant k \leqslant 13$
	$-17 \leqslant l \leqslant 16$	$-16 \leqslant l \leqslant 16$	$-77 \leqslant l \leqslant 93$	$-59 \leqslant l \leqslant 90$
Measured reflections	17510	11638	8333	9073
Independent reflections	6766	5761	2053	1977
Independant reflections with $I > 3\sigma$	4471	2484	1246	1274
μ(mm^{-1})	8.594	10.054	12.008	8.403
3. *Structure solution and refinement*				
Parameters refined	179	202	61	62
Agreement factors	$R = 3.09\%$; $Rw = 3.35\%$	$R = 4.46\%$; $Rw = 4.02\%$	$R = 2.80\%$; $Rw = 2.94\%$	$R = 2.89\%$; $Rw = 3.21\%$
weighting scheme	$w = 1/(\sigma(F)^2 + 1.10^{-4}\,F^2)$	$w = 1/(\sigma(F)^2)$	$w = 1/(\sigma(F)^2 + 1 \times 10^{-4}\,F^2)$	$w = 1/(\sigma(F)^2 + 1 \times 10^{-4}F^2)$
Δ/σ max	1.1×10^{-3}	8.0×10^{-3}	6.7×10^{-3}	4.1×10^{-3}

O(12), respectively. The final refinement of atomic coordinates for all atoms (including hydrogen atoms), with anisotropic displacement parameters for Cs, In, P and O atoms and isotropic displacement parameters for hydrogen atoms, led to reliability factors $R = 0.0309$ and $Rw = 0.0335$. The corresponding atomic coordinates, equivalent isotropic thermal parameters and their estimated standard deviations are listed in Table 2a.

The structure of α-$RbFe(PO_3(OH))_2$ **(2)** was refined in the triclinic space group $P\bar{1}$, starting from the structural model determined for $CsIn(PO_3(OH))_2$. The Rb, Fe, P and O atoms were introduced with the atomic parameters previously determined for Cs, In, P and O, respectively. The refinement of these parameters confirmed that the structure of α-$RbFe(PO_3(OH))_2$ was isotypic with that of $CsIn(PO_3(OH))_2$. However, a quite strong electronic residue ($2.44\,e^-.Å^{-3}$) was observed on the Fourier difference map at 0.12 Å from Rb(2). This residue was no more observed after the introduction of fourth order anharmonic tensors for Rb(2). It was thus possible to localize the hydrogen atoms, using the same method as mentioned above for compound **1**. Their isotropic atomic displacement parameters were refined but constrained to adopt the same value. All other atoms were refined anisotropically, leading to the reliability factors $R = 4.47\%$ and $Rw = 3.71\%$ and to the atomic parameters listed in Table 2b.

The structure of compound **3**, $RbGa(PO_3(OH))_2$, was solved in the centrosymmetric $R\bar{3}c$ space group, hexagonal setting, in agreement with the conditions for the observed reflections. The structure determination was performed using the heavy atom method and successive Fourier and difference Fourier maps. The positions of all Rb, Ga, P and O atoms were refined anisotropically, leading to the reliability factors $R = 2.94\%$ and $Rw = 3.26\%$. The bond valence sum calculation led to the expected values for all atoms of compound **3** except O(4) for which a value of 1.38 (instead of 2) was obtained. This result indicates the

Table 2a
Positional parameters, atomic displacement parameters and their estimated standard deviations in $CsIn(PO_3(OH))_2$ **(1)**

Atom	x	y	z	$U_{eq.}$ (Å^2)
Cs(1)	1	1	0	0.02513(13)
Cs(2)	0.86458(4)	0.83452(3)	0.47178(2)	0.02386(9)
In(1)	0.5	0.5	0.5	0.00740(8)
In(2)	0.70231(3)	0.71589(2)	−0.049760(19)	0.00754(6)
P(1)	0.59077(11)	0.34474(9)	0.21648(8)	0.0079(2)
P(2)	0.40787(11)	0.87928(9)	0.23393(8)	0.0078(2)
P(3)	0.95329(11)	0.55245(9)	0.22480(7)	0.0075(2)
O(1)	0.4488(3)	0.4174(3)	0.3414(2)	0.0132(8)
O(2)	0.3446(3)	0.7479(3)	0.3856(2)	0.0136(7)
O(3)	0.7793(4)	0.5412(3)	0.3619(2)	0.0174(8)
O(4)	0.6636(4)	0.4734(3)	0.0699(2)	0.0144(8)
O(5)	0.4625(3)	0.8202(3)	0.0982(2)	0.0136(8)
O(6)	0.9028(3)	0.6806(3)	0.0751(2)	0.0123(7)
O(7)	0.5088(3)	0.7615(3)	−0.1924(2)	0.0122(7)
O(8)	0.7550(3)	0.9577(3)	−0.2107(2)	0.0102(7)
O(9)	0.9439(3)	0.6224(3)	−0.2147(2)	0.0107(7)
O(10)	0.7771(4)	0.2125(3)	0.2790(3)	0.0152(8)
O(11)	0.5927(4)	0.9201(3)	0.2453(3)	0.0171(9)
O(12)	1.0992(4)	0.6200(3)	0.2574(3)	0.0173(9)
H(10)	0.856(7)	0.259(6)	0.267(5)	0.016(11)
H(11)	0.565(7)	1.018(6)	0.236(5)	0.019(11)
H(12)	1.203(7)	0.570(6)	0.272(5)	0.026(13)

The atomic displacement parameters of hydrogen atoms were refined isotropically (U_{iso}). The atomic displacement parameters of all other atoms were refined anisotropically and are given in the form of an equivalent isotropic displacement parameter defined by $U_{eq} = \frac{1}{3}\sum_{i=1}^{3}\sum_{i=1}^{3} U_{ij}a^{*i}a^{*j}\vec{a}_i\vec{a}_j$.

Table 2b
Positional parameters, atomic displacement parameters and their estimated standard deviations in α-$RbFe(PO_3(OH))_2$ **(2)**

Atom	x	y	Z	$U_{eq.}$ (Å^2)
Rb(1)	1	1	0	0.0303(3)
Rb(2)	0.86299(16)	0.83274(12)	0.47574(12)	0.0377(6)
Fe(1)	0.5	0.5	0.5	0.0068(3)
Fe(2)	0.70499(7)	0.71581(6)	−0.05115(6)	0.00652(18)
P(1)	0.58963(13)	0.34665(10)	0.21734(11)	0.0064(3)
P(2)	0.41440(13)	0.87777(10)	0.23267(11)	0.0066(3)
P(3)	0.94890(13)	0.55580(11)	0.22190(11)	0.0060(3)
O(1)	0.4465(4)	0.4170(3)	0.3494(3)	0.0105(10)
O(2)	0.3458(4)	0.7401(3)	0.3891(3)	0.0098(9)
O(3)	0.7622(4)	0.5415(3)	0.3587(3)	0.0123(10)
O(4)	0.6681(4)	0.4828(3)	0.0681(3)	0.0106(10)
O(5)	0.4753(4)	0.8176(3)	0.0913(3)	0.0102(10)
O(6)	0.9015(4)	0.6860(3)	0.0640(3)	0.0092(9)
O(7)	0.5157(4)	0.7559(3)	−0.1874(3)	0.0103(10)
O(8)	0.7530(3)	0.9547(3)	−0.2066(3)	0.0091(9)
O(9)	0.9367(3)	0.6243(3)	−0.2157(3)	0.0091(9)
O(10)	0.7782(4)	0.2044(3)	0.2794(3)	0.0115(10)
O(11)	0.6025(4)	0.9183(3)	0.2484(4)	0.0150(12)
O(12)	1.0863(4)	0.6313(4)	0.2617(4)	0.0151(12)
H(10)	0.870(6)	0.256(5)	0.261(5)	0.005(7)
H(11)	0.573(6)	0.987(5)	0.248(5)	0.005(7)
H(12)	1.170(6)	0.594(5)	0.263(6)	0.005(7)

All atoms were refined with harmonic displacement parameters, except Rb(2) which was refined with fourth-order anharmonic displacement parameter and hydrogen atoms which were refined isotropically (U_{iso}) and constrained to adopt the same value. The non-hydrogen atoms are given in the form of an equivalent isotropic displacement parameter U_{eq} defined by $U_{eq} = \frac{1}{3}\sum_{i=1}^{3}\sum_{i=1}^{3} U_{ij}a^{*i}a^{*j}\vec{a}_i\vec{a}_j$.

existence of one hydroxyl group on O(4), leading to the formula $RbGa(PO_3(OH))_2$ for compound **3**. The corresponding hydrogen atom was localized using the same method as mentioned above for compound **1**. Its position was refined, leading to a O(4)–H(4) distance of 0.77(3)Å, and a position toward the O(3) atom consistent with usual hydrogen bonding geometry. The final refinement of the atomic parameters, including anisotropic displacement parameters for Rb, Ga, P and O atoms and isotropic one for H(4) led to the reliability factors $R = 2.80\%$ and $Rw = 2.94\%$ for $RbGa(PO_3(OH))_2$. The corresponding atomic coordinates, equivalent isotropic thermal parameters and their estimated standard deviations are listed in Table 2c.

Table 2c
Positional parameters, atomic displacement parameters and their estimated standard deviations in $RbGa(PO_3(OH))_2$ **(3)**

Atom	x	y	z	$U_{eq.}$ (Å^2)
Rb(1)	0	0	0.75	0.02134(13)
Rb(2)	0	0	0.666412(6)	0.02518(11)
Ga(1)	0.3333	0.6667	0.6667	0.00791(10)
Ga(2)	0.3333	0.6667	0.752785(5)	0.00715(7)
P(1)	0.02978(7)	0.41520(7)	0.712715(7)	0.00734(15)
O(1)	0.1044(2)	0.5147(2)	0.68730(2)	0.0140(5)
O(2)	0.18101(19)	0.44065(19)	0.73214(2)	0.0100(5)
O(3)	−0.11373(19)	0.46841(19)	0.72335(2)	0.0091(4)
O(4)	−0.0868(2)	0.1936(2)	0.70675(3)	0.0139(5)
H(4)	−0.190(4)	0.157(4)	0.7110(5)	0.030(8)

The atomic displacement parameters of hydrogen atoms were refined isotropically (U_{iso}). The atomic displacement parameters of all other atoms were refined anisotropically and are given in the form of an equivalent isotropic displacement parameter defined by $U_{eq} = \frac{1}{3}\sum_{i=1}^{3}\sum_{i=1}^{3} U_{ij}a^{*i}a^{*j}\vec{a}_i\vec{a}_j$.

The structural model of $RbGa(PO_3(OH))_2$ was used for the structure determination of compound **4**, since the same space group ($R\bar{3}c$) and similar cell parameters were observed. The refinement of the atomic parameters of Rb, Al, P and O atoms led to the reliability factors $R = 3.06\%$ and $Rw = 3.49\%$ for compound **4**, confirming that its structure is isotypic with that of $RbGa(PO_3(OH))_2$. However, a quite important residual electronic density ($1.75\,e^-\,Å^{-3}$) was observed at 0.55 Å of Rb(1) on the difference Fourier map. Third order anharmonic displacement parameters were thus introduced for this atom. The refinement led then to better reliability factors ($R = 3.02\%$ and $Rw = 3.44\%$) and no more significant electronic residue was observed (maximum of $0.9\,e.Å^{-3}$). As for $RbGa(PO_3(OH))_2$, the bond valence sum calculation led to the expected values for all atoms except for O(4) (1.41 instead of 2), indicating that an hydroxyl group was present on this atom. The corresponding H(4) atom was

located in the structure using the same method as mentioned above for compounds **1**, **2** and **3**. It was refined to be at 0.79(4) Å of O(4), with a position toward O(3) coherent with usual hydrogen bonding geometry. The final refinement of the atomic parameters, including anisotropic displacement parameters for Rb, Al, P and O atoms and isotropic one for H(4) led to the reliability factors $R = 2.89\%$ and $Rw = 3.21\%$ for $RbAl(PO_3(OH))_2$. The corresponding atomic coordinates, equivalent isotropic thermal parameters and their estimated standard deviations are listed in Table 2d.

Table 2d
Positional parameters, atomic displacement parameters and their estimated standard deviations in $RbAl(PO_3(OH))_2$ **(4)**

Atom	x	y	z	$U_{eq.}$ (Å^2)
Rb(1)	0	0	0.75	0.02053(11)
Rb(2)	0	0	0.665993(6)	0.02172(9)
Al(1)	0.3333	0.6667	0.6667	0.0056(2)
Al(2)	0.3333	0.6667	0.753647(15)	0.00544(17)
P(1)	0.03306(6)	0.42167(6)	0.712882(8)	0.00569(13)
O(1)	0.11090(16)	0.52533(17)	0.68744(2)	0.0102(4)
O(2)	0.18290(15)	0.44881(15)	0.73306(2)	0.0074(4)
O(3)	−0.11780(15)	0.46838(16)	0.72339(2)	0.0073(4)
O(4)	−0.08058(18)	0.19884(18)	0.70641(3)	0.0119(4)
H(4)	−0.188(5)	0.166(5)	0.7102(6)	0.054(10)

All atoms were refined with harmonic displacement parameters, except Rb(1) which was refined with third-order anharmonic displacement parameter and H(4) which was refined isotropically. The non-hydrogen atoms are given in the form of an equivalent isotropic displacement parameter U_{eq} defined by $U_{eq} = \frac{1}{3}\sum_{i=1}^{3}\sum_{i=1}^{3} U_{ij} a^{*i} a^{*j} \vec{a}_i \vec{a}_j$.

Further details of the crystal structure investigations (including anisotropic displacement parameters and Fo–Fc lists) can be obtained from the Fachinformationszentrum Karlsruhe, 76344 Eggenstein-Leopoldshafen, Germany (fax: (49) 7247-808-666; e-mail: crysdata@fiz.karlsruhe.de), on quoting the following depository numbers: CSD-417706 for $CsIn(PO_3(OH))_2$, CSD-417707 for $RbFe(PO_3(OH))_2$, CSD-417708 for $RbAl(PO_3(OH))_2$, and CSD-417709 for $RbGa(PO_3(OH))_2$.

4. Results and discussion

The four studied hydroxyphosphates "Cs–In", α-"Rb–Fe", "Rb–Ga" and "Rb–Al" correspond to two

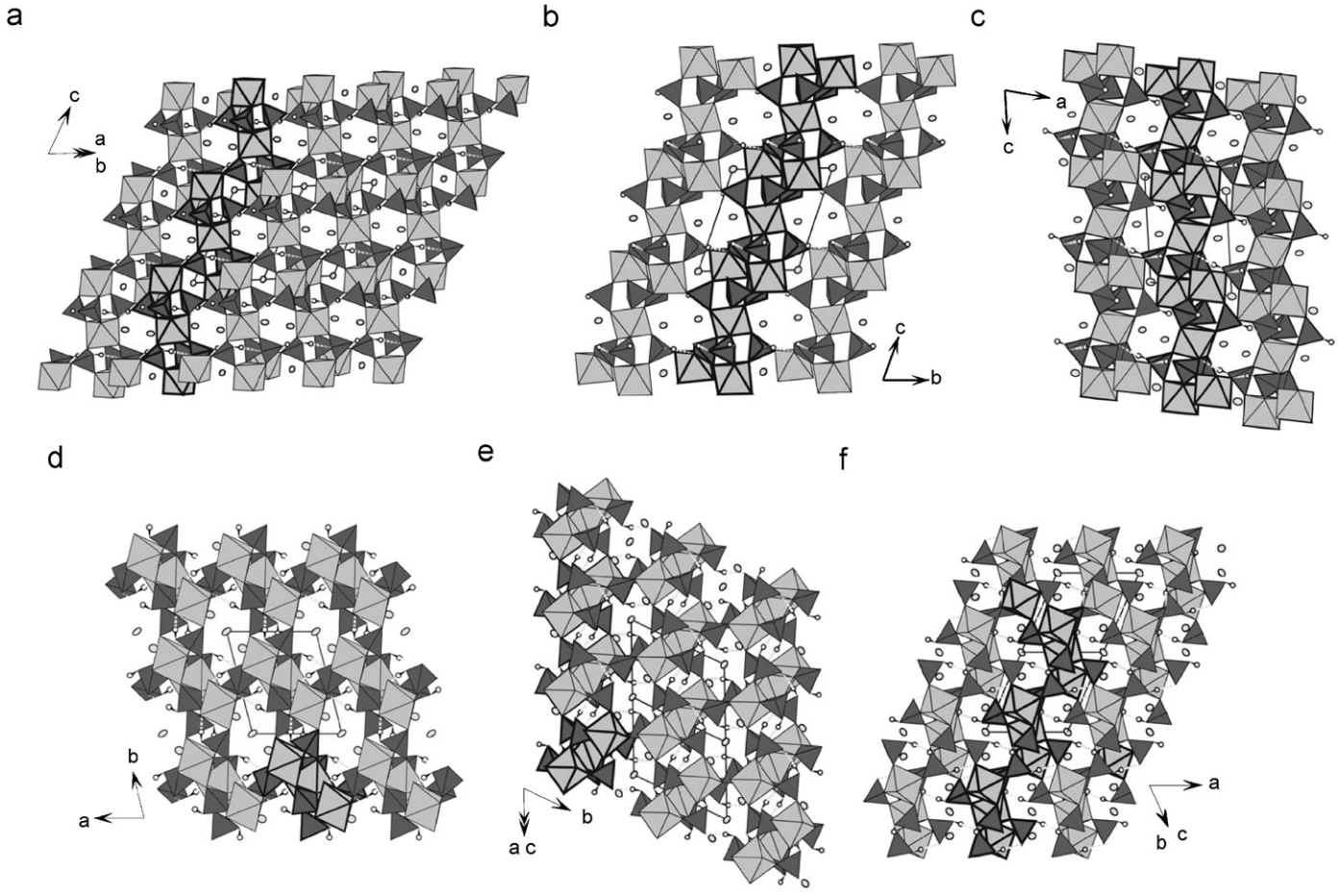

Fig. 1. Projections of the triclinic structure type ($CsIn(PO_3(OH))_2$ and $RbFe(PO_3(OH))_2$), showing the $[M_3O_4(PO_3(OH))_6]_\infty$ columns (bold lines) and the different tunnels (a) along $[1\bar{1}0]$, (b) along [100], (c) along [010], (d) along $[00\bar{1}]$, (e) along $[\bar{1}01]$ and (f) along $[0\bar{1}1]$. The MO_6 octahedra (M = In, Fe) are medium-grey. The dark-grey tetrahedra correspond to the PO_4 groups, the hydrogen atoms of the hydroxyl groups being represented as white circles. The hydrogen bonds are symbolized by dotted lines. The monovalent cations (Cs or Rb) are represented with their displacement ellipsoids, drawn at 70% probability level (light-grey).

different intersecting tunnels structures, as evidenced by the comparison of the projections of the two structural types (Figs. 1 and 2). The "Cs–In" and the "Rb–Fe" hydroxyphosphates crystallize indeed with a triclinic symmetry (Fig. 1), their structure being isotypic with α-$RbV(HPO_4)_2$, $NH_4V(HPO_4)_2$, $NH_4(Al_{0.64}Ga_{0.36})(HPO_4)_2$, $H_3OAl(HPO_4)_2$ and $NH_4Fe(PO_3(OH))_2$ [15–19]. The "Rb–Ga" and "Rb–Al" hydroxyphosphates present a trigonal symmetry (described here in an hexagonal cell), which has already been observed for another form of $RbFe(HPO_4)_2$ [20] (Fig. 2). Although they have different symmetries, the two structure types exhibit close relationships. Both $[M^{III}(PO_3(OH))_2]_\infty$ host-lattices are indeed built from similar $M_3O_6[PO_3(OH)]_6$ structural units, in which three $M^{III}O_6$ octahedra (M = In, Al, Ga, Fe) share their apices with six $PO_3(OH)$ tetrahedra (Fig. 3). The central MO_6 octahedron of the centrosymmetric $M_3O_6[PO_3(OH)]_6$ unit shares its six apices with the six hydroxyphosphate groups, whereas each of the two other octahedra shares three apices with three $PO_3(OH)$ tetrahedra of its own building unit, and three other apices with the $PO_3(OH)$ tetrahedra belonging to three other building units (Fig. 3). As a consequence, each monophosphate group of one unit shares two of its apices with two MO_6 octahedra of its own building unit, its third apex with one MO_6 octahedron of an adjacent building unit, whereas its fourth apex, which corresponds to the hydroxyl group, is free (Fig. 3). In spite of these similarities, the configuration of the $M_3O_6[PO_3(OH)]_6$ structural units encountered in the triclinic form (Fig. 3a and b) is significantly different from that of the trigonal form (Fig. 3c and d). Clearly, the relative orientations of the polyhedra, and especially that of the $PO_3(OH)$ tetrahedra are not the same in the two structural types.

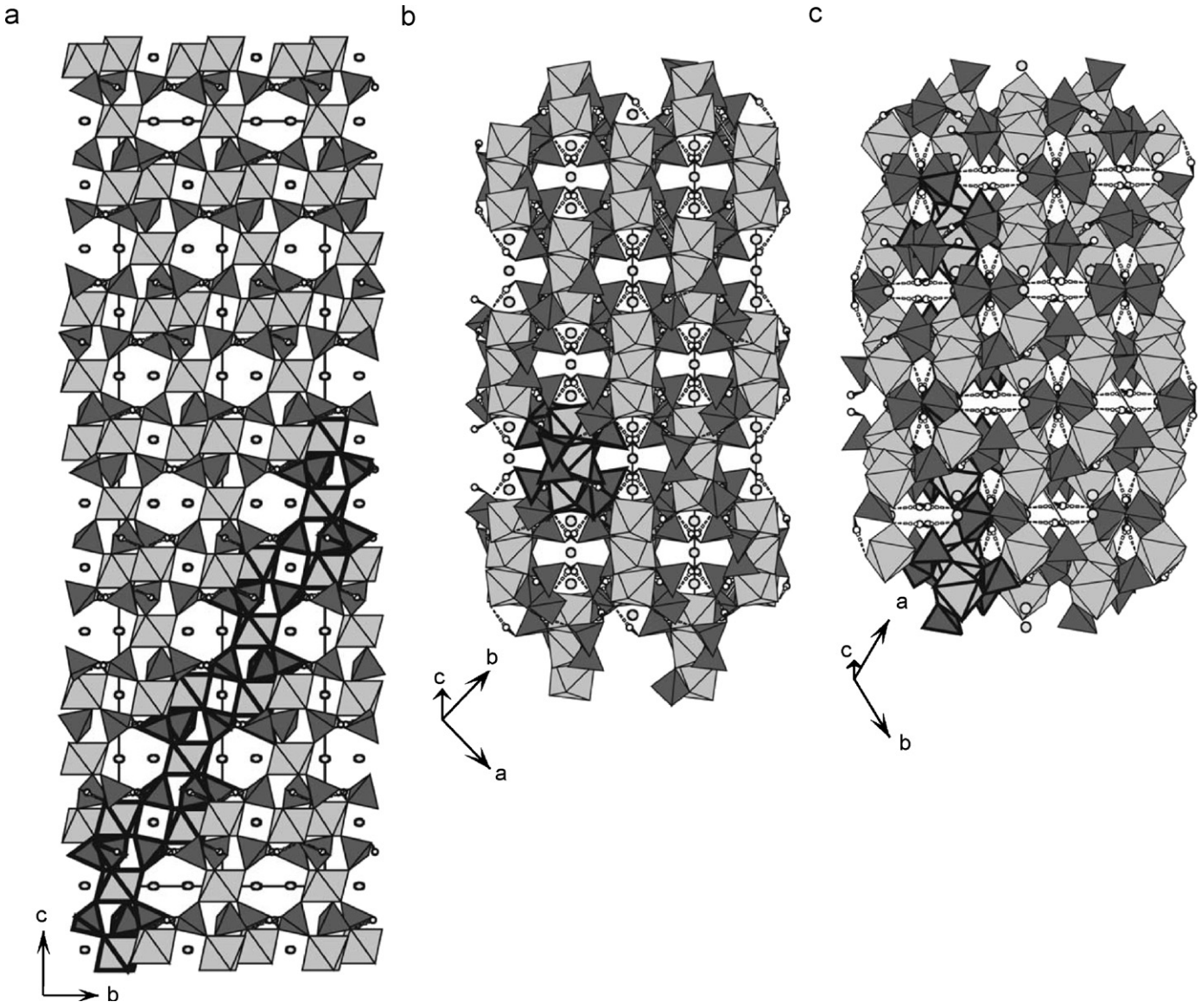

Fig. 2. Projections of the trigonal structure type ($RbAl(PO_3(OH)_2$ and $RbGa(PO_3(OH)_2$) (a) along $[\bar{1}\bar{1}0]$, (b) along $[2\bar{2}1]$, and (c) along $[\bar{1}\bar{1}1]$. The medium-grey octahedra correspond to AlO_6 or GaO_6. See Fig. 1 for complete legend.

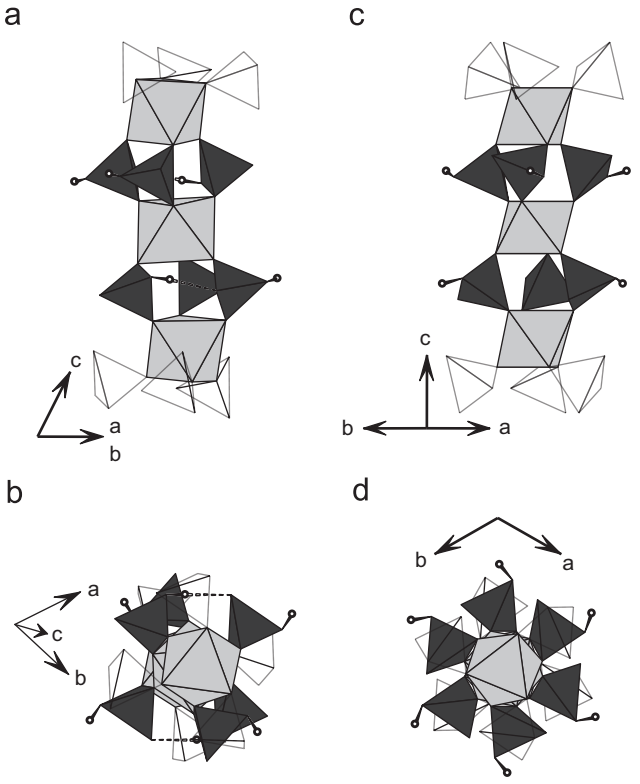

Fig. 3. Projections of one $M_3O_6[PO_3(OH)]_6$ structural unit (a) along $[1\bar{1}0]$ in the triclinic structure type, (b) along $[11\bar{3}]$ in the triclinic structure type, (c) along $[\bar{1}\bar{1}0]$ in the trigonal structure type, and (d) along $[00\bar{1}]$ in the trigonal structure type. The white tetrahedra correspond to the hydroxymonophosphate groups belonging to adjacent $M_3O_6[PO_3(OH)]_6$ structural units. See Figs. 1 and 2 for complete legend.

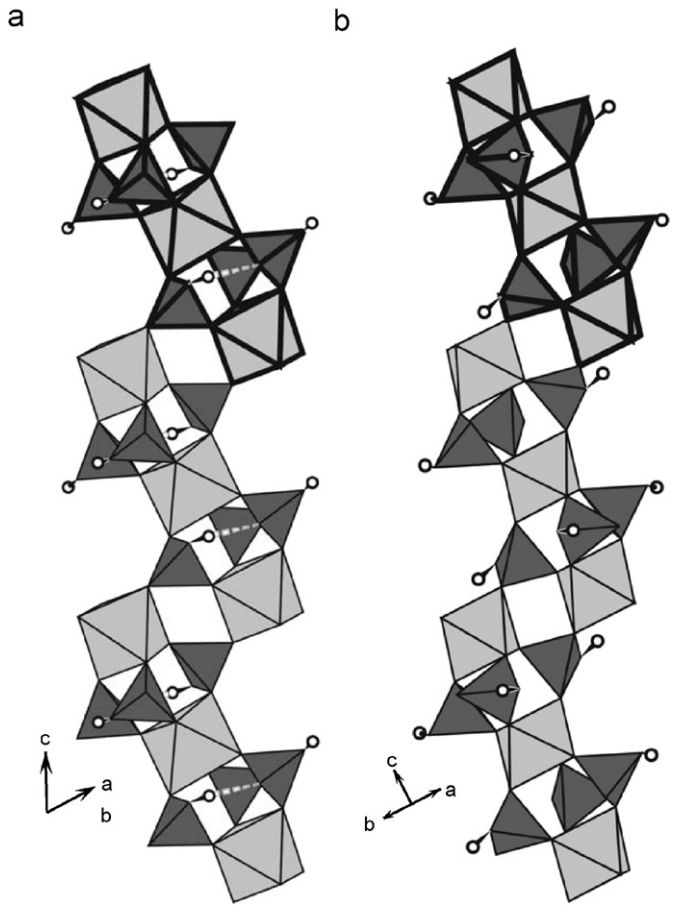

Fig. 4. Projection of one $[M_3O_4[PO_3(OH)]_6]_\infty$ column built from $M_3O_6[PO_3(OH)]_6$ structural units (a) along $[1\bar{1}0]$ in the triclinic structure type ($CsIn(PO_3(OH))_2$ and $RbFe(PO_3(OH))_2$), and (b) along $[\bar{1}\bar{1}0]$ in the trigonal structure type ($RbAl(PO_3(OH)_2$ and $RbGa(PO_3(OH)_2$). One $M_3O_6[PO_3(OH)]_6$ structural unit has been drawn with bold lines on each projection. See Figs. 1 and 2 for complete legend.

However, in both structural types, the $M_3O_6[PO_3(OH)]_6$ units are connected to form $[M_3O_4[PO_3(OH)]_6]_\infty$ columns (Fig. 4). In the triclinic three-dimensional framework, the $[M_3O_4[PO_3(OH)]_6]_\infty$ columns (Fig. 4a) are parallel to [001] and assembled along **a** and **b** through the corners of their polyhedra (Fig. 1). The $[M_3O_4[PO_3(OH)]_6]_\infty$ columns observed in the trigonal form (Fig. 4b) are running along the $[2\bar{2}1]$ direction of the hexagonal cell (Fig. 2). The most obvious difference between the two studied frameworks types comes from these columns. In the triclinic form, two successive $M_3O_6[PO_3(OH)]_6$ units of a $[M_3O_4[PO_3(OH)]_6]_\infty$ column are identical, one being deduced from the other through a simple $\vec{c}$ shift (Fig. 4a), whereas in the trigonal form they are deduced one from the other through a 180° rotation around the two-fold axis parallel to the [110] direction (Fig. 4b). This explains the larger cell volume of the trigonal form (ca. 2900 Å^3) in regard with the triclinic form (ca. 500 Å^3). However, in both three-dimensional $[M^{III}(PO_3(OH))_2]_\infty$ host-lattices, each $[M_3O_4[PO_3(OH)]_6]_\infty$ column shares the apices of its polyhedra with four similar columns, this assemblage giving rise to numerous intersecting tunnels (Figs. 1–2).

One remarkable feature of these structures deals indeed with the exceptionally open character of their frameworks. However, since the orientation of the polyhedra which form the $M_3O_6[PO_3(OH)]_6$ basic unit is not the same in the triclinic and in the trigonal forms, the tunnels generated by the junction of these units present different shapes in the two host-lattices. In the triclinic host-lattice, one can observe at least four types of tunnels containing the monovalent cation: (i) eight-sided tunnels delimited by four octahedra and four tetrahedra, running along **a** (Fig. 1b), along **b** (Fig. 1c), and more distorted ones running along $[10\bar{1}]$ (Fig. 1a), (ii) large elliptic tunnels running along **c** (Fig. 1d), (iii) six-sided tunnels delimited by two octahedra and four tetrahedra running along $[1\bar{1}0]$ (Fig. 1e), and (iv) S-shaped tunnels running along $[0\bar{1}1]$ (Fig. 1f). In the trigonal form, there are six-sided tunnels parallel to the $\langle 100 \rangle$ (and consequently along $\langle 110 \rangle$) directions (Fig. 2a), cross-shaped tunnels running along $[2\bar{2}1]$ (Fig. 2b) and butterfly-shaped tunnels running along $[\bar{1}11]$ (Fig. 2c).

The geometries observed for the different polyhedra of the four studied compounds are in agreement with those usually observed in literature. The average values for the M^{III}–O distances are 2.136 Å for In–O in $CsIn(PO_3(OH))_2$, 2.005 Å for Fe–O in α-$RbFe(PO_3(OH))_2$, 1.963 Å for Ga–O

in $RbGa(PO_3(OH))_2$ and 1.898 Å for Al–O in $RbAl(PO_3(OH))_2$. The average P–O distances are of 1.538, 1.536, 1.538 and 1.537 Å in the indium, iron, gallium and aluminium hydroxymonophosphates, respectively.

As expected, the $M(1)$ octahedron (located at the centre of the $M_3O_6[PO_3(OH)]_6$ structural unit) is more regular than the $M(2)$ one. The bonds between $M(2)$ and the three oxygen atoms belonging to the same building unit (O(4), O(5) and O(6) in the triclinic structures, O(2) in the trigonal form) are indeed significantly shorter than the bonds involving oxygen atoms shared between two units (O(7), O(8) and O(9) in the triclinic form and O(3) in the trigonal one). More particularly, in the triclinic structure, the O(8) atom seems to be far from its ideal position, leading to the largest $M(2)$–O bond (Table 3) and to the most distorted O–$M(2)$–O(8) angles.

Concerning the geometry of the hydroxymonophosphate groups, as expected, the P–OH bonds are the largest ones (mean values of 1.587 Å vs 1.520 Å for the P–O distances). The O–H bonds of the hydroxyl groups are short, with a mean distance value of 0.74 Å, i.e. similar to those previously reported in literature, for instance in other indium hydroxymonophosphates [24,25]. More importantly, these hydroxyl groups point toward the nearest oxygen atoms available to form strong hydrogen bonds with distances ranging from 1.79(5) to 2.23(4) Å and O–H···O angles close to 180° (from 163(5) to 177(3)°) (Table 3). This small deviation is attributed to the presence of the non-bonding orbitals of oxygen atoms. These hydrogen bonds, which are all approximately perpendicular to the $[M_3O_4[PO_3(OH)]_6]_\infty$ columns, contribute to the stability and to the configuration of the framework. In the triclinic form, H(10) points indeed toward O(9) inside the same building units (Fig. 3a and 3b) whereas H(11) and H(12) point toward oxygen atoms of other building units (O(7) and O(1), respectively) (Fig. 1). In the trigonal form, the H(4) atoms point toward the O(3) atoms of adjacent units (Fig. 2). These observations justify the above description of the $[M(PO_3(OH))_2]_\infty$ frameworks in terms of $[M_3O_4[PO_3(OH)]_6]_\infty$ columns. In the triclinic host-lattice for instance, the columns are parallel to c, and the cohesion of the three-dimensional host-lattice is reinforced by the existence of hydrogen bonds, besides the role of the monovalent cations.

Table 3a
Selected bond distances (Å) in $CsIn(PO_3(OH))_2$ **(1)**

In(1)–O(1) = 2.163(3)	
In(1)–O(1^{i}) = 2.163(3)	
In(1)–O(2) = 2.1517(19)	Cs(1)–O(6) = 2.971(3)
In(1)–O(2^{i}) = 2.1517(19)	Cs(1)–O(6^{v}) = 2.971(3)
In(1)–O(3) = 2.117(2)	Cs(1)–O(11) = 3.254(2)
In(1)–O(3^{i}) = 2.117(2)	Cs(1)–O(11^{v}) = 3.254(2)
	Cs(1)–O(12) = 3.330(2)
In(2)–O(4) = 2.095(2)	Cs(1)–O(12^{v}) = 3.330(2)
In(2)–O(5) = 2.091(2)	Cs(1)–O(8) = 3.374(3)
In(2)–O(6) = 2.092(3)	Cs(1)–O(8^{v}) = 3.374(3)
In(2)–O(7) = 2.155(3)	Cs(1)–O(5^{vi}) = 3.517(2)
In(2)–O(8) = 2.186(2)	Cs(1)–O(5^{iii}) = 3.517(2)
In(2)–O(9) = 2.1567(19)	Cs(1)–O(10^{iv}) = 3.606(3)
	Cs(1)–O(10^{vii}) = 3.606(3)
P(1)–O(1) = 1.533(2)	
P(1)–O(4) = 1.498(2)	
P(1)–O(7^{ii}) = 1.529(3)	Cs(2)–O(9^{viii}) = 3.0006(19)
P(1)–O(10) = 1.591(2)	Cs(2)–O(10^{vii}) = 3.113(2)
	Cs(2)–O(12) = 3.127(3)
P(2)–O(2) = 1.5166(19)	Cs(2)–O(11) = 3.175(3)
P(2)–O(5) = 1.514(3)	Cs(2)–O(2^{vi}) = 3.249(2)
P(2)–O(8^{iii}) = 1.537(2)	Cs(2)–O(1^{i}) = 3.370(3)
P(2)–O(11) = 1.588(4)	Cs(2)–O(7^{viii}) = 3.4261(19)
	Cs(2)–O(8^{viii}) = 3.479(3)
P(3)–O(3) = 1.510(2)	Cs(2)–O(3) = 3.561(3)
P(3)–O(6) = 1.516(2)	Cs(2)–O(8^{v}) = 3.591(2)
P(3)–O(9^{iv}) = 1.533(2)	Cs(2)–O(3^{ix}) = 3.646(2)
P(3)–O(12) = 1.584(4)	

	O–H	O–H···O	H···O
O(10)–H(10)– O(9^{iv})	0.79(6)	174(5)	1.94(6)
O(11)– H(11)– O(7^{iii})	0.81(5)	172(6)	1.79(5)
O(12)– H(12)– O(1^{vi})	0.77(5)	170(4)	2.00(5)

Symmetry codes: (i) 1−x, 1−y, 1−z; (ii) 1−x, 1−y, −z; (iii) 1−x, 2−y, −z; (iv) 2−x, 1−y, −z; (v) 2−x, 2−y, −z; (vi) 1+x, y, z; (vii) x, 1+y, z; (viii) x, y, 1+z; (ix) 2−x, 1−y, 1−z.

Table 3b
Selected bond distances (Å) in α-$RbFe(PO_3(OH))_2$ **(2)**

Fe(1)–O(1) = 2.039(4)	
Fe(1)–O(1^{i}) = 2.039(4)	
Fe(1)–O(2) = 2.0280(19)	Rb(1)–O(6) = 2.869(3)
Fe(1)–O(2^{i}) = 2.0280(19)	Rb(1)–O(6^{v}) = 2.869(3)
Fe(1)–O(3) = 1.958(2)	Rb(1)–O(11) = 3.107(3)
Fe(1)–O(3^{i}) = 1.958(2)	Rb(1)–O(11^{v}) = 3.107(3)
	Rb(1)–O(12) = 3.158(3)
Fe(2)–O(4) = 1.950(2)	Rb(1)–O(12^{v}) = 3.158(3)
Fe(2)–O(5) = 1.954(2)	Rb(1)–O(8) = 3.264(3)
Fe(2)–O(6) = 1.951(3)	Rb(1)–O(8^{v}) = 3.264(3)
Fe(2)–O(7) = 2.030(3)	Rb(1)–O(10^{iv}) = 3.448(3)
Fe(2)–O(8) = 2.070(2)	Rb(1)–O(10^{vii}) = 3.448(3)
Fe(2)–O(9) = 2.049(2)	Rb(1)–O(5^{vi}) = 3.473(3)
	Rb(1)–O(5^{iii}) = 3.473(3)
P(1)–O(1) = 1.527(3)	
P(1)–O(4) = 1.503(2)	Rb(2)–O(9^{viii}) = 2.833(3)
P(1)–O(7^{ii}) = 1.522(4)	Rb(2)–O(12) = 2.941(4)
P(1)–O(10) = 1.581(3)	Rb(2)–O(10^{vii}) = 2.974(2)
	Rb(2)–O(11) = 3.016(4)
P(2)–O(2) = 1.522(2)	Rb(2)–O(2^{vi}) = 3.173(3)
P(2)–O(5) = 1.514(3)	Rb(2)–O(1^{i}) = 3.228(3)
P(2)–O(8^{iii}) = 1.535(2)	Rb(2)–O(7^{viii}) = 3.283(2)
P(2)–O(11) = 1.583(4)	Rb(2)–O(8^{viii}) = 3.360(3)
	Rb(2)–O(8^{v}) = 3.528(3)
P(3)–O(3) = 1.513(2)	Rb(2)–O(3) = 3.551(4)
P(3)–O(6) = 1.515(2)	Rb(2)–O(3^{ix}) = 3.602(2)
P(3)–O(9^{iv}) = 1.531(3)	
P(3)–O(12) = 1.577(4)	

	O–H	O–H···O	H···O
O(10)–H(10)–O(9^{iv})	0.86(5)	178(3)	1.87(5)
O(11)–H(11)–O(7^{iii})	0.57(5)	165(6)	2.01(4)
O(12)–H(12)–O(1^{vi})	0.58(4)	162(5)	2.22(4)

Symmetry codes: (i) 1−x, 1−y, 1−z; (ii) 1−x, 1−y, −z; (iii) 1−x, 2−y, −z; (iv) 2−x, 1−y, −z; (v) 2−x, 2−y, −z; (vi) 1+x, y, z; (vii) x, 1+y, z; (viii) x, y, 1+z; (ix) 2−x, 1−y, 1−z.

Table 3c
Selected bond distances (Å) in $RbGa(PO_3(OH))_2$ **(3)**

Ga(1)–O(1) = 1.9576(12)	Rb(1)–O(4) = 3.0204(17)
Ga(1)–O(1^{i}) = 1.9576(12)	Rb(1)–O(4^{ix}) = 3.0204(16)
Ga(1)–O(1^{ii}1.958(2)	Rb(1)–O(4x) = 3.0204(17)
Ga(1)–O(1^{iii}) = 1.958(2)	Rb(1)–O(4^{xi}) = 3.0204(19)
Ga(1)–O(1^{iv}) = 1.9576(15)	Rb(1)–O(4vii) = 3.0204(19)
Ga(1)–O(1^{v}) = 1.9576(15)	Rb(1)–O(4^{xii}) = 3.0204(16)
	Rb(1)–O(2) = 3.2499(14)
Ga(2)–O(2) = 1.9436(12)	Rb(1)–O(2^{ix}) = 3.2499(13)
Ga(2)–O(2^{ii}) = 1.9436(14)	Rb(1)–O(2x) = 3.2499(14)
Ga(2)–O(2^{iv}) = 1.9436(19)	Rb(1)–O(2^{vxii}) = 3.2499(13)
Ga(2)–O(3^{vi}) = 1.9908(12)	Rb(1)–O(2^{xi}) = 3.250(2)
Ga(2)–O(3^{vii}) = 1.9908(13)	Rb(1)–O(2vii) = 3.250(2)
Ga(2)–O(3^{viii}) = 1.9908(19)	
	Rb(2)–O(4) = 2.9095(18)
P(1)–O(1) = 1.5075(12)	Rb(2)–O(4^{ix}) = 2.9095(16)
P(1)–O(2) = 1.5212(15)	Rb(2)–O(4^{xi}) = 2.9095(19)
P(1)–O(3) = 1.5338(19)	Rb(2)–O(1^{xiii}) = 3.2691(15)
P(1)–O(4) = 1.5890(16)	Rb(2)–O(1^{xiv}) = 3.269(3)
	Rb(2)–O(1^{v}) = 3.2691(13)
	Rb(2)–O(3^{xiii}) = 3.3190(12)
	Rb(2)–O(3^{xiv}) = 3.3190(14)
	Rb(2)–O(3^{v}) = 3.3190(12)
	Rb(2)–O(4^{xii}) = 3.4414(19)
	Rb(2)–O(4^{xiv}) = 3.441(2)
	Rb(2)–O(4^{v}) = 3.4414(18)

	O–H	O–H···O	H···O
O(4)–H(4)–O(3^{xv})	0.77(3)	169(3)	1.82(5)

Symmetry codes: (i) 2/3−x, 4/3−y, 4/3−z; (ii) 1−y, 1+x−y, z; (iii) −1/3+y, 1/3−x+y, 4/3−z; (iv) −x+y, 1−x, z; (v) 2/3+x−y, 1/3+x, 4/3−z; (vi) y, 1+x, 3/2−z; (vii) −x, −x+y, 3/2−z; (viii) 1+x−y, 1−y, 3/2−z; (ix) −y, x−y, z; (x) y, x, 3/2−z; (xi) −x+y, −x, z; (xii) x−y, −y, 3/2−z; (xiii) −1/3−x, 1/3−y, 4/3−z; (xiv) −1/3+y, −2/3−x+y, 4/3−z; (xv) −1−x+y, −x, z.

Table 3d
Selected bond distances (Å) and angles (°) in $RbAl(PO_3(OH))_2$ **(4)**

Al(1)–O(1) = 1.8958(10)	Rb(1)–O(4) = 2.9977(15)
Al(1)–O(1^{i}) = 1.8958(10)	Rb(1)–O(4^{ix}) = 2.9977(14)
Al(1)–O(1^{ii}) = 1.8958(17)	Rb(1)–O(4x) = 2.9977(15)
Al(1)–O(1^{iii}) = 1.8958(17)	Rb(1)–O(4^{xi}) = 2.9977(16)
Al(1)–O(1^{iv}) = 1.8958(12)	Rb(1)–O(4vii) = 2.9977(16)
Al(1)–O(1^{v}) = 1.8958(12)	Rb(1)–O(4^{xii}) = 2.9977(14)
	Rb(1)–O(2) = 3.2666(11)
Al(2)–O(2) = 1.8787(11)	Rb(1)–O(2^{ix}) = 3.2666(10)
Al(2)–O(2^{ii}) = 1.8787(13)	Rb(1)–O(2x) = 3.2666(11)
Al(2)–O(2^{iv}) = 1.8787(16)	Rb(1)–O(2^{xi}) = 3.2666(18)
Al(2)–O(3^{vi}) = 1.9200(11)	Rb(1)–O(2vii) = 3.2666(18)
Al(2)–O(3^{vii}) = 1.9200(12)	Rb(1)–O(2^{vxii}) = 3.2666(10)
Al(2)–O(3^{viii}) = 1.9200(16)	
	Rb(2)–O(4) = 2.8796(15)
P(1)–O(1) = 1.5021(11)	Rb(2)–O(4^{ix}) = 2.8796(14)
P(1)–O(2) = 1.5178(13)	Rb(2)–O(4^{xi}) = 2.8796(17)
P(1)–O(3) = 1.5379(15)	Rb(2)–O(3^{xiii}) = 3.2417(11)
P(1)–O(4) = 1.5899(13)	Rb(2)–O(3^{xiv}) = 3.2417(13)
	Rb(2)–O(3^{v}) = 3.2417(11)
	Rb(2)–O(1^{xiii}) = 3.2747(12)
	Rb(2)–O(1^{v}) = 3.2747(11)
	Rb(2)–O(1^{xiv}) = 3.275(2)
	Rb(2)–O(4^{xii}) = 3.3932(16)
	Rb(2)–O(4^{xiv}) = 3.3932(17)
	Rb(2)–O(4^{v}) = 3.3932(15)

	O–H	O–H···O	H···O
O(4)–H(4)–O(3^{xv})	0.79(4)	170(3)	1.79(4)

Symmetry codes: (i) 2/3−x, 4/3−y, 4/3−z; (ii) 1−y, 1+x−y, z; (iii) −1/3+y, 1/3−x+y, 4/3−z; (iv) −x+y, 1−x, z; (v) 2/3+x−y, 1/3+x, 4/3−z; (vi) y, 1+x, 3/2−z; (vii) −x, −x+y, 3/2−z; (viii) 1+x−y, 1−y, 3/2−z; (ix) −y, x−y, z; (x) y, x, 3/2−z; (xi) −x+y, −x, z; (xii) x−y, −y, 3/2−z; (xiii) −1/3−x, 1/3−y, 4/3−z; (xiv) −1/3+y, −2/3−x+y, 4/3−z; (xv) −1−x+y, −x, z.

The monovalent cations sit at the intersections of the previously mentioned tunnels. The *A*(1) cations present a twelve-fold coordination corresponding to six O and six OH neighbours, whatever the structure type. As expected, the coordination polyhedra observed for *A*(1) cations are more distorted in the triclinic structures than in the trigonal ones. One indeed observes for the triclinic compounds Cs(1)–O distances comprised between 2.971(3) Å and 3.606(3) Å in $CsIn(PO_3(OH)_2)$ and Rb(1)–O distances ranging from 2.868(3) Å to 3.447(3) Å in α-RbFe $(PO_3(OH)_2$, whereas the Rb(1)–O distances in the two trigonal phosphates are much more homogeneous, ranging from 3.0204(19) Å to 3.250(2) Å in $RbGa(PO_3(OH)_2)$ and from 2.9977(16) Å to 3.2666(18) Å in $RbAl(PO_3(OH)_2)$. The *A*(2) cations have also a twelve-fold coordination in the trigonal structure, but it is less regular than for *A*(1). It corresponds to six oxygen atoms and six hydroxyl groups, with Rb(2)–O distances ranging from 2.9095(18) Å to 3.4414(18) Å and from 2.8796(15) Å to 3.3932(17) Å in the gallium and aluminium compounds, respectively. Finally, in the triclinic structure type, the *A*(2) cation is surrounded by 8 oxygen atoms and 3 hydroxyl groups, with Cs(2)–O distances ranging from 3.0006(19) Å to 3.646(2) Å in $CsIn(PO_3(OH)_2)$ and Rb(2)–O distances ranging from 2.833(3) Å to 3.602(2) Å in α-RbFe $(PO_3(OH)_2$ (Table 3).

The existence of several compounds for each of the two structural types studied in this paper allows to analyze the influence of the monovalent A and trivalent *M* cations on the structural characteristics. The triclinic host-lattice appears to be more flexible, since it is observed for various *A* and *M* cations. It can indeed exist with H_3O^+ and Al for the smallest ones [18] and also with Cs^+ and In for the largest ones (this work) (Table 4). On the opposite, the trigonal form has only been reported for the rubidium cation associated to trivalent elements of similar sizes i.e. Al, Ga (this work) or Fe [20].

The possibility to obtain for the composition RbFe $(PO_3(OH)_2$ either the triclinic structure (this work) or the trigonal one [20] allows the comparison of the Fe–Fe distances in the two framework types. The Fe(1)–Fe(2) distances in a $[M_3O_4[PO_3(OH)]_6]_\infty$ column are rather similar in the two forms, with values of 4.560 Å in the trigonal form and 4.6140 Å in the triclinic one. The main difference is observed for the Fe–Fe distances between two iron atoms of two adjacent columns, with ca. 4.72 Å in the trigonal form versus ca. 5.18 Å in the triclinic one. This has to be related to the different configurations observed

Table 4
Cristallographic characteristics of the different $AM(HPO_4)_2$ compounds observed for the two structural types (triclinic and trigonal)

Compound	Space group	Z	a (Å)	b (Å)	c (Å)	α (°)	β (°)	γ (°)	V (Å^3)
$NH_4(Al_{0.64}Ga_{0.36})(HPO_4)_2$	$P\bar{1}$	3	7.109(4)	8.695(4)	9.252(6)	65.01(4)	70.25(5)	69.01(4)	472.1(4)
$H_3OAl(HPO_4)_2$	$P\bar{1}$	3	7.1177(2)	8.6729(2)	9.2200(3)	65.108(2)	70.521(1)	68.504(2)	469.4(2)
α-RbFe(HPO$_4$)$_2$	$P\bar{1}$	3	7.2025(4)	8.8329(8)	9.4540(8)	65.149(8)	70.045(6)	69.591(6)	497.44(8)
α-$NH_4V(HPO_4)_2$	$P\bar{1}$	3	7.173(2)	8.841(2)	9.458(2)	65.08(2)	70.68(2)	69.59(2)	497.7(2)
$NH_4Fe(HPO_4)_2$[a]	$P\bar{1}$	3	7.185(3)	8.857(3)	9.478(3)	64.79(3)	70.20(3)	69.38(3)	498.0(3)
α-$RbV(HPO_4)_2$	$P\bar{1}$	3	8.831(1)	9.450(2)	7.188(2)	109.55(2)	110.26(1)	65.34(1)	498.5(2)
CsIn(HPO$_4$)$_2$	$P\bar{1}$	3	7.4146(3)	9.0915(3)	9.7849(3)	65.525(3)	70.201(3)	69.556(3)	547.77(4)
RbAl(HPO$_4$)$_2$	$R\bar{3}c$	18	8.0581(18)	8.0581(18)	51.081(12)	90	90	120	2872.5(11)
RbGa(HPO$_4$)$_2$	$R\bar{3}c$	18	8.1188(15)	8.1188(15)	51.943(4)	90	90	120	2965.1(8)
$RbFe(HPO_4)_2$	$R\bar{3}c$	18	8.160(1)	8.160(1)	52.75(1)	90	90	120	3041.82

The compounds reported in the present paper are in bold characters. The bibliographic references of the others compounds are given in the text.
[a]The structure of $NH_4Fe(HPO_4)_2$ was initially reported in the $I\bar{1}$ space group, with $Z = 6$. The cell parameters given by the authors (space group $I\bar{1}$, $Z = 6$) have been transformed into the reduced cell ($P\bar{1}$, $Z = 3$) in order to facilitate the comparison with the other compounds.

for the hydroxymonophosphate groups in the $M_3O_6[PO_3(OH)]_6$ structural units, which induce a different relative disposition of the $[M_3O_4[PO_3(OH)]_6]_\infty$ columns in the two frameworks.

In conclusion, this study and the results obtained by previous authors [15–20] show the extraordinary ability of the *A*–*M*–P–O–H system to form two closely related intersecting tunnel structures for hydroxyphosphates with the generic formula $AM(PO_3(OH))_2$. The most numerous series deals with the Rb phases which can be synthesized either in the triclinic form for $M = V$, Fe or in the trigonal form for $M = Ga$, Al, Fe. The existence of two forms for the same cation $M = Fe$, shows the great flexibility of such structural types. It is worth pointing out that hydronium and ammonium cations seem to exhibit a similar behaviour, as shown by the existence of the triclinic "H_3O–Al" [18] and "NH_4–V" [16] hydroxyphosphates. One remarkable feature deals with the fact that a cesium hydroxyphosphate is obtained for the first time. Moreover it must be emphasized that in the latter case, the presence of a larger cation in the octahedral sites, i.e. indium, seems to be necessary to stabilize the structure. Note also that a different monoclinic structure has previously been observed for "Rb–V" and "NH_4–V" hydroxyphosphates with the same formula [15,16]. Further studies should thus be performed in order to have a better understanding of the different parameters which determine the structural type adopted for a given chemical composition. Moreover, these studies could lead to determine new structural types for compounds of general formula $AM(PO_3(OH))_2$.

Acknowledgment

Authors gratefully acknowledge the Région Basse-Normandie and the Ministère de la Recherche for financial support.

References

[1] A.D. Robertson, A.R. West, A.G. Ritchie, Solid State Ion. 104 (1997) 1–11.
[2] A.K. Padhi, K.S. Nanjundaswamy, J.B. Goodenough, J. Electrochem. Soc. 144 (1997) 1188–1194.
[3] P.P. Prosini, M. Lisis, S. Scaccia, M. Carewska, F. Cardelline, M. Pasquali, J. Electrochem. Soc. 149 (2002) A297–A301.
[4] S.Y. Chung, J.T. Bloking, Y.M. Chiang, Nat. Mater. 1 (2002) 123–128.
[5] M.E. Davis, R.F. Lobo, Chem. Mater. 4 (1992) 756–768.
[6] M.E. Davis, Nature 417 (2002) 813–821.
[7] G. Centy, F. Trifiro, J.R. Ebner, V.M. Franchetti, Chem. Rev. 88 (1988) 55–60.
[8] M. Ai, K. Ohdan, J. Mol. Catal. A 159 (2000) 19–24.
[9] R.C. Ewing, W.J. Webert, F.W. Clinard, Prog. Nucl. Energy 29-2 (1995) 63–127.
[10] J. Carpena, J.L. Lacout, L'Actualité Chim 2 (1997) 3.
[11] L.M. Wang, J. Chen, R.C. Ewing, Curr. Opin. Solid State Mater. Sci. 8 (2004) 405–418.
[12] Y. Zhang, W. Cheng, D.-S. Wu, H. Zhang, D. Chen, Y. Gong, Z. Kan, Chem. Mater. 16 (16) (2004) 4150–4159.
[13] E.V. Murashova, N.N. Chudinova, Izv. Akad. Nauk, Neorg. Mater. 37 (12) (2001) 1521–1524.
[14] S.S. Dhingra, R.C. Haushalter, J. Solid State Chem. 112 (1994) 96–99.
[15] R.C. Haushalter, Z.-W. Wang, M.E. Thompson, J. Zubieta, Inorg. Chim. Acta 232 (1995) 83–89.
[16] Z. Bircsak, W.T.A. Harrison, Acta Crystallogr. C 54 (1998) 1195–1197.
[17] S.M. Stalder, A.P. Wilkinson, J. Mater. Chem. 8 (1) (1998) 261–263.
[18] W. Yan, J. Yu, Z. Shi, R. Xu, Chem. Comm. (2000) 1431–1432.
[19] O.V. Yakubovich, Kristallografiya 38 (5) (1993) 43–48.
[20] K.-H. Lii, L.-S. Wu, J. Chem. Soc. Dalton Trans. (1994) 1577–1580.
[21] A.J.M. Duisenberg, L.M.J. Kroon-Batenburg, A.M.M. Schreurs, J. Appl. Crystallogr. 36 (2003) 220.
[22] V. Petricek, M. Dusek, The crystallographic computing system JANA 2000, Institute of Physics, Praha, Czech Republic, 2000.
[23] N.E. Brese, M. O'Keeffe, Acta Crystallogr. B 47 (1991) 192–197.
[24] J.X. Mi, Y.X. Huang, S.Y. Mao, X.D. Huang, Z.B. Wei, Z.L. Huang, J.T. Zhao, J. Solid State Chem. 157 (2001) 213–219.
[25] X. Tang, A. Jones, A. Lachgar, B.J. Gross, J.L. Yarger, Inorg. Chem. 38 (1999) 6032–6038.